



## Tropical rainfall-surface temperature relations using Tropical Rainfall Measuring Mission precipitation data

Jian-Jian Wang,<sup>1,2</sup> Robert F. Adler,<sup>2,3</sup> and Guojun Gu<sup>1,2</sup>

Received 25 October 2007; revised 9 June 2008; accepted 13 June 2008; published 30 September 2008.

[1] In this study, 9 years (1998–2006) of monthly precipitation data from Tropical Rainfall Measuring Mission (TRMM) are used to examine the relations between tropical rainfall and surface temperature using measurements from both passive and active microwave sensors. These relations are compared to those derived from Global Precipitation Climatology Project (GPCP) analyses. A technique is first developed to adjust the TRMM Precipitation Radar (PR) monthly rainfall data in the tropics (whole ocean and whole land) to account for the effect of the TRMM orbit boost from 350 to 402 km in August 2001. The postboost PR rainfall is adjusted by adding 6.5, 6.0, and 1.0% to the monthly PR rainfall data over the ocean at the estimated surface, the near surface, and the 2 km level, respectively. No adjustment is made for data over land or above the 4 km level. The relationships between the tropical rainfall and surface temperature are then examined with both the TRMM Microwave Imager (TMI) and adjusted PR data. Comparing tropical (25°N–25°S) ocean precipitation to mean sea surface temperature (SST) over the same area, the GPCP and TMI rainfall data have large and similar slopes ( $\sim 15\%/^{\circ}\text{C}$ ) against ocean-wide SST anomalies, while the surface monthly rainfall anomalies derived from the TRMM PR exhibit much shallower slopes ( $\sim 4\%/^{\circ}\text{C}$ ) against the SST anomalies. At the 4 km level the PR data exhibit a larger slope ( $12\%/^{\circ}\text{C}$ ) comparable to the passive microwave value. Over the tropical land, all rainfall data except TRMM PR at 6 km have similar, but negative, slopes against surface temperature anomalies, in contrast to the positive slopes over the ocean. Over the total tropics (ocean and land combined), TRMM TMI and GPCP rainfall data have rather similar smaller positive slopes ( $6\%/^{\circ}\text{C}$ ), when compared to ocean plus land surface temperature, but the PR rainfall data slopes are slightly negative, except at the 4 km level ( $4\%/^{\circ}\text{C}$ ). Overall, the PR-based surface precipitation-temperature slopes do not confirm slopes based on passive microwave observations. This may be the result of PR retrieval error or inherent passive/active retrieval differences. Further research is needed to advance the use of TRMM data in this regard.

**Citation:** Wang, J.-J., R. F. Adler, and G. Gu (2008), Tropical rainfall-surface temperature relations using Tropical Rainfall Measuring Mission precipitation data, *J. Geophys. Res.*, *113*, D18115, doi:10.1029/2007JD009540.

### 1. Introduction

[2] Tropical convection and its associated precipitation are key components to the Earth's water cycle. Long-term analyses of global precipitation data such as that from the Global Precipitation Climatology Project (GPCP) [Adler *et al.*, 2003a] are used to investigate regional and global precipitation variations on time scales from seasonal to interdecadal. Interannual variations in the tropics are dominated by the El Niño-Southern Oscillation (ENSO)

phenomenon, although its influence on precipitation patterns can be shown to have a global reach [Soden, 2000; Curtis and Adler, 2003].

[3] In terms of longer time-scale variations, Gu *et al.* [2007] isolate the ENSO precipitation signal and the signal related to volcanic aerosols, allowing a better examination of the remaining long-term linear changes (i.e., trends) over the 1979–2005 period in the tropics. These calculated linear changes show a 5% increase over tropical oceans during the 27-year period and a slight decrease over land, resulting in a possible 4% increase over the tropics as a whole. A similar increase in ocean precipitation has also been noted by Wentz *et al.* [2007], using passive microwave rain retrievals for a shorter period. This estimated precipitation increase is coincident with increased surface temperatures over both ocean and land. The GPCP interannual and long-term precipitation changes over the ocean are primarily driven by information based on Special Sensor Microwave/Imager

<sup>1</sup>Goddard Center for Earth Science and Technology, University of Maryland Baltimore County, Catonsville, Maryland, USA.

<sup>2</sup>Laboratory for Atmospheres, NASA Goddard Space Flight Center, Greenbelt, Maryland, USA.

<sup>3</sup>Earth System Science Interdisciplinary Center, University of Maryland, College Park, Maryland, USA.

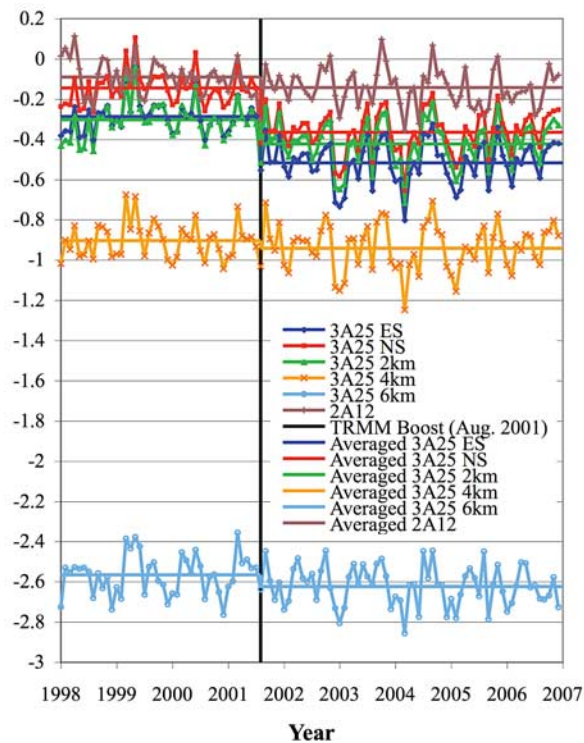


**Figure 1.** Time series of the difference between PR (3A25) and GPCP monthly rainfall data at selected levels. The solid black line indicates the time when the TRMM satellite raised its orbit.

(SSM/I) data on polar-orbiting satellites (for a full description of GPCP data and techniques, see *Adler et al.* [2003a]). Passive microwave retrievals over the ocean require information about the depth of the rain column, which is usually tied to the height of the  $0^{\circ}\text{C}$  isotherm, which, in turn, is correlated to surface temperature [e.g., *Chiu and Chang*, 2000; *Kummerow et al.*, 2001]. Hence, interannual or long-term rain-temperature relations using rain variations deduced from passive microwave observations must be used cautiously since temperature information (directly or indirectly) is necessary for the rain retrievals. With the launch of the Tropical Rainfall Measuring Mission (TRMM) [*Simpson*, 1988; *Kummerow et al.*, 2000] satellite in late 1997, it is now possible to examine variations in rainfall with information from both the TRMM Microwave Imager (TMI) (passive microwave) and the TRMM Precipitation Radar (PR), albeit for a relatively short period (<10 years). Rain retrievals based on the PR are independent of surface or tropospheric temperature. The objective of this research is to examine surface temperature-precipitation relations over the tropics with both the active and passive microwave sensors on TRMM and compare the results to GPCP-based calculations to seek confirmation of these relations.

## 2. Satellite Data Sets

[4] TRMM-based rainfall retrievals (version 6) from the TMI (TRMM algorithm product number 2A12) [*Kummerow et al.*, 2001] and from the PR (2A25) [*Iguchi et al.*, 2000] are

used for the 9-year period 1998–2006. Our analysis will use the TMI-based monthly mean values of surface rainfall and monthly values of rain at the estimated surface (ES), the near surface (NS), and the 2, 4, and 6 km levels from the PR. The gridded monthly averages are provided at  $0.5^{\circ} \times 0.5^{\circ}$  resolutions covering roughly  $38^{\circ}\text{S}$  to  $38^{\circ}\text{N}$ . However, focusing on the tropical region in this study, we only use data from  $25^{\circ}\text{S}$  to  $25^{\circ}\text{N}$ .

[5] The GPCP monthly precipitation data set is a community-based analysis of global precipitation under the auspices of the World Climate Research Program (WCRP) from 1979 to the present [*Adler et al.*, 2003a]. On a global  $2.5^{\circ} \times 2.5^{\circ}$  grid, the data are combined from the following information sources: microwave-based estimates from SSM/I, infrared (IR) rainfall estimates from geostationary and polar-orbiting satellites, and surface rain gauges. The analysis procedure is designed to take advantage of particular strengths of the individual input data sets, especially in terms of bias reduction. For example, the microwave information is used to adjust the bias of the IR-based estimates over the ocean and land, and the gauge information is used to adjust the bias of the merged satellite estimates over land. Therefore, the data set should have the low bias of the input information deemed to be best, with the superior sampling on a monthly scale produced by multiple satellites. The period from 1988 to the present is homogeneous in terms of input data sets. Further information about the GPCP monthly data set is detailed by *Adler et al.* [2003a] and *Huffman et al.* [1997].

[6] The NASA Goddard Institute for Space Studies (GISS) monthly temperature product is on a  $1^{\circ} \times 1^{\circ}$  grid. It combines air temperature anomalies from meteorological station measurements over land and sea surface temperature (SST) information [*Hansen et al.*, 1999]. The SST data set is based on satellite infrared measurements during the post-1981 period [*Reynolds et al.*, 2002] and, therefore, is independent from the precipitation estimation. Details are shown by *Hansen et al.* [1999], and the product can be obtained through the NASA GISS Web site.

## 3. Adjustment of PR Rain Estimates for Impact of Orbit Boost

[7] Before the PR rain estimates for the entire 9-year period can be used in this analysis, the impact of the TRMM orbit boost from 350 to 402 km altitude in 2001 must be taken into account. The effect of the boost is shown in Figure 1, where the time series of PR monthly rainfall data relative to the monthly GPCP rainfall for the latitude band  $25^{\circ}\text{N}$ – $25^{\circ}\text{S}$  is plotted. Because the GPCP is only a surface rain estimate and the different PR products are at different altitudes with a general decrease with height, the important value is the change in the offset from before to after the boost. The GPCP analysis does not contain TRMM data and is, therefore, independent of the boost effects. There is an apparent drop of PR rainfall estimates at the lower levels (especially at ES and NS levels (Figure 1)) since August 2001, when TRMM's orbit was raised to extend the mission's life. It is also noted that this drop of the PR rainfall amount during the postboost period is less obvious at 2 km, with only about half of the decrease at the surface. At the 4 and 6 km levels, the difference between TRMM

**Table 1.** Mean Differences Between TRMM Rainfall Measurements and GPCP Before and After the Boost of TRMM Satellite<sup>a</sup>

	Mean Difference (mm/d)			Significance Level (%)
	Preboost Period	Postboost Period	Postboost Minus Preboost	
3A25 estimated surface	-0.29	-0.52	-0.23	99.95
3A25 near surface	-0.15	-0.37	-0.22	99.94
3A25 2 km	-0.30	-0.42	-0.12	99.58
3A25 4 km	-0.90	-0.94	-0.04	92.74
3A25 6 km	-2.57	-2.62	-0.05	96.79
2A12	-0.09	-0.14	-0.05	97.00

<sup>a</sup>The preboost period is January 1998 to August 2001; the postboost period September 2001 to December 2006. TRMM, Tropical Rainfall Measuring Mission; GPCP, Global Precipitation Climatology Project.

3A25 and GPCP remains about the same from the preboost to postboost period (Figure 1). These results are also consistent with the studies by *Robertson et al.* [2007]. Table 1 gives the shift in the mean values from before to after the boost (relative to GPCP). The PR value at the ES level drops 0.23 mm/d. Relative to the preboost mean PR ES value (2.6 mm/d) this is a drop of over 8.8%. This type of decrease must be taken into account when using the PR data for careful interannual studies. A Student's *t* test has been performed to evaluate the significance level of the difference between preboost and postboost periods to the variance of the monthly rainfall. The results are shown in the last column of Table 1. For the purpose of developing a technique to adjust the TRMM postboost monthly rainfall, we would like to have the significance level not less than 99%. As shown in Table 1, the significance levels of the ES, NS, and 2 km PR monthly products are all above 99.5% and much higher than those of the TMI (2A12), 4 km, and 6 km PR monthly products. The TMI (2A12) algorithm was adjusted for field of view size change for retrievals after the orbit altitude increase. On the basis of the results from Figure 1 and Table 1, we have developed postboost adjustments for the ES, NS, and 2 km PR monthly products.

[8] *Takahashi and Iguchi* [2004] state that the effect of the TRMM orbit boost on the PR data may include (1) the degradation of the radar sensitivity by about 1.2 dB due to the larger distance from satellite to rain target and (2) a mismatch between the transmission and reception angles for 1 pulse from among 32 pulses. Using PR nadir data, *Kwiatkowski et al.* [2007] suggested that the increased thickness of clutter region due to the orbit boost may be the main factor responsible for the decrease of PR rain near the surface.

[9] In this study, we first develop a simple and robust technique for adjusting the PR monthly rainfall data in the tropics (whole ocean and whole land) during the postboost period to make PR rainfall data a homogenous data set. The basis for the adjustment approach is that there are two main factors influencing the estimated monthly ocean (and land) TRMM PR retrievals. The first is the impact of the orbit boost as already described. The second is the relationship between the tropical ocean (and land) rainfall and ENSO events [e.g., *Soden, 2000; Gu et al., 2007*]. Ocean and land are treated separately because of small but significant differences in PR retrievals over land and ocean and also differences in the TMI-based rain retrievals between ocean and land. In this exercise, the Nino3.4 index will be used as

an indicator of ENSO events. Nino3.4 is the average sea surface temperature anomaly in the region bounded by 5°N to 5°S, from 170° to 120°W, which is the region with most intense variability on interannual/El Niño time scales.

[10] To study the relationship between monthly rainfall anomalies and the Nino3.4 index, the seasonal variation of rainfall is first removed. Ideally, a complete monthly climatology of rainfall from January to December throughout the 9-year (1998–2006) TRMM period would be calculated as the mean state. However, since the 9-year averaged PR data contain both preboost and postboost periods, the GPCP rainfall data were selected for this purpose. The difference of the monthly TRMM PR rainfall from the GPCP monthly climatology of rainfall from January to December is then treated as the monthly rainfall anomaly. The difference in relation between rainfall anomaly and the Nino3.4 index for the preboost and postboost periods of TRMM satellite will provide the basis for adjusting the postboost period monthly rainfall for tropical ocean and land.

[11] To confirm and increase our confidence on the adjustment of PR data, rainfall data from Defense Meteorological Satellite Program (DMSP) F13 satellite were also used to replace GPCP rainfall data as the climatological reference for PR rainfall data. Then an analysis similar to the one using the GPCP data is performed. The F13 satellite has a very stable equatorial crossing time (~1800 local standard time (LST)) throughout the entire 9-year period, which removes the possible effects of diurnal cycle. However, a drawback of F13 rainfall data is that over land, the F13 rainfall is much higher than other estimations from GPCP, TRMM PR, and TMI. Therefore, F13 rainfall data are only used for the PR rainfall analysis over the ocean.

[12] The PR monthly rainfall anomalies over the tropical ocean versus the Nino3.4 index anomalies for the preboost and postboost periods are shown in Figure 2. The linear regression line for the preboost period (1998–2001) has a relatively steep slope, while the linear regression line for the postboost period (2001–2006) is nearly flat, indicating that the correlation is near zero and there is little or no relation between ENSO (Nino3.4) and PR ocean rainfall during the postboost period. Another interesting feature in Figure 2 is that for the preboost period, Nino3.4 swings from large negative (La Niña) to large positive (El Niño) numbers. The preboost period went from a strong El Niño during the first few months of 1998 to a strong La Niña for most of the rest of the period up to August 2001. On the other hand, for the postboost period, Nino3.4 has a small range centered on

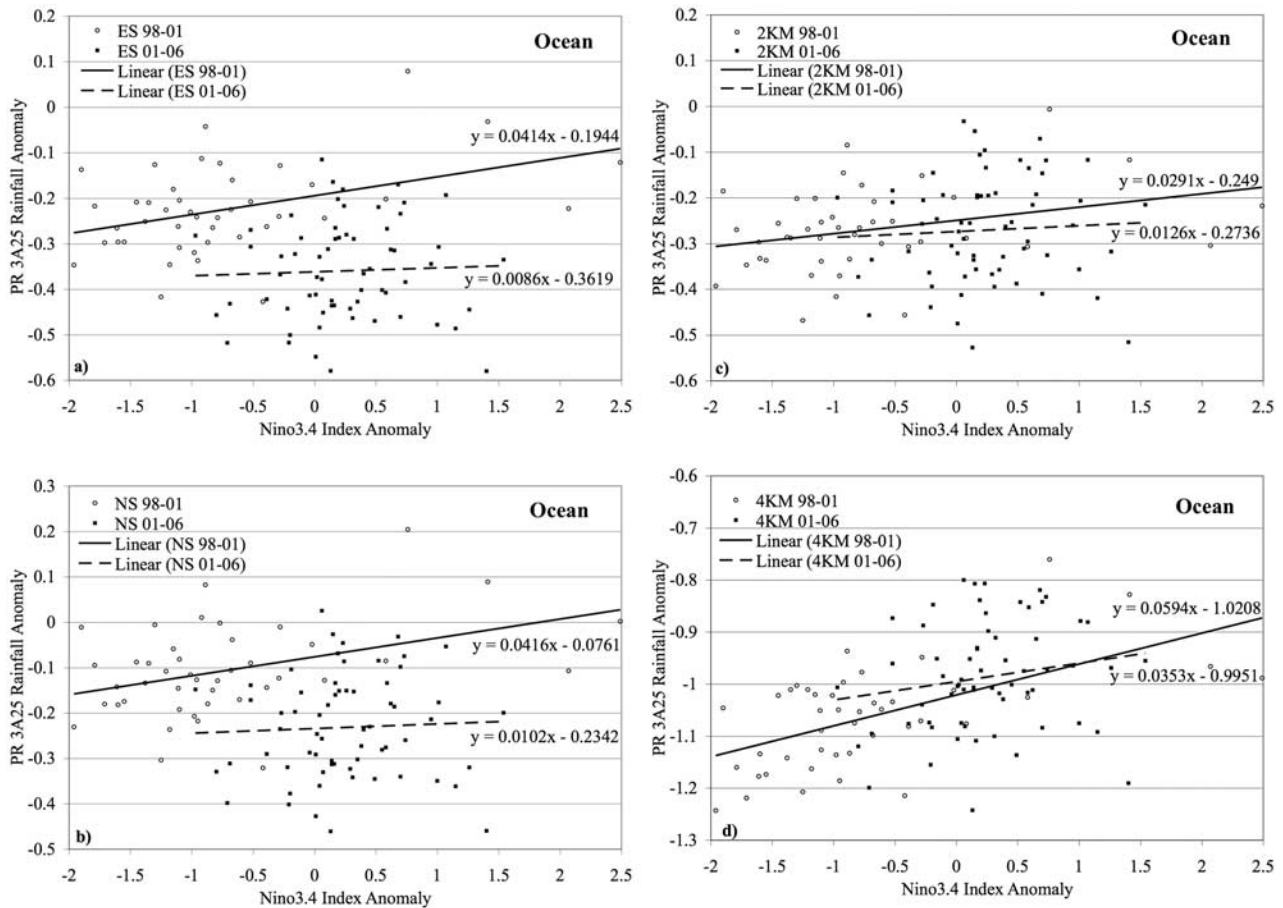


**Figure 2.** The PR rainfall anomalies (mm/d) over the tropical ocean (25°S–25°N) versus Nino3.4 index at (a) estimated surface, (b) near surface, (c) 2 km, and (d) 4 km.

neutral conditions. This relatively small range may partially contribute to the lack of correlation between PR rainfall anomalies and Nino3.4 during the later period. Despite the relatively strong slope for the preboost period and the relatively flat regression line for the postboost period, our hypothesis that the two linear regression lines have a significant gap with the rainfall anomalies for the postboost period at a lower value compared to that for the preboost period is confirmed. The results also seem to confirm that the ENSO phase should be taken into account. Figure 2 also shows the significant gap between the linear regression lines for preboost and postboost periods for the lowest levels (Figures 2a and 2b) and a reduced gap at the 2 km level (Figure 2c). The gap disappears at the 4 km level (Figure 2d) and above (not shown).

[13] On the basis of these results, a procedure to adjust the mean PR-based monthly rainfall over the tropical ocean for the postboost period was determined. The differences between the monthly rainfall anomalies for the postboost period (September 2001 to December 2006), indicated by the 64 squares (Figure 2), and the preboost period, indicated by the solid linear regression lines (Figure 2), are calculated. Corresponding to the same Nino3.4 index, the mean PR rainfall during the postboost period is calculated to be 6.5, 6.0, and 1.0% less than that of the preboost period for the

ES, NS, and 2 km levels, respectively. To confirm these results, we also use F13 rainfall data to replace GPCP rainfall data as the climatological reference for PR data and repeat the above analysis. The results match the previous analysis very well, with the mean PR rainfall during the postboost period being about 6.6, 6.0, and 1.1% less than that of the preboost period at the ES, NS, and 2 km levels, respectively, using the SSM/I estimates as a reference. This increases our confidence to make the adjustment for PR data during the postboost period over the tropical ocean.

[14] A similar analysis is also performed for the PR monthly rainfall data over the tropical land using GPCP rainfall data (Figure 3) for the climatology. For the preboost period (1998–2001), which contains both strong La Niña events and strong El Niño events, the PR rainfall anomalies over the tropical land show a clear negative correlation with Nino3.4 anomalies as expected. However, for the postboost period (2001–2006), which contains mostly near-neutral years, the correlation between the PR rainfall anomalies and Nino3.4 anomalies is less significant. In contrast to the PR rainfall relations over tropical ocean shown in Figure 2, the regression lines for the preboost period and postboost period rainfall anomalies over tropical land cross each other in the middle of Figure 3 (Nino3.4 index range of 0.5 to –0.5

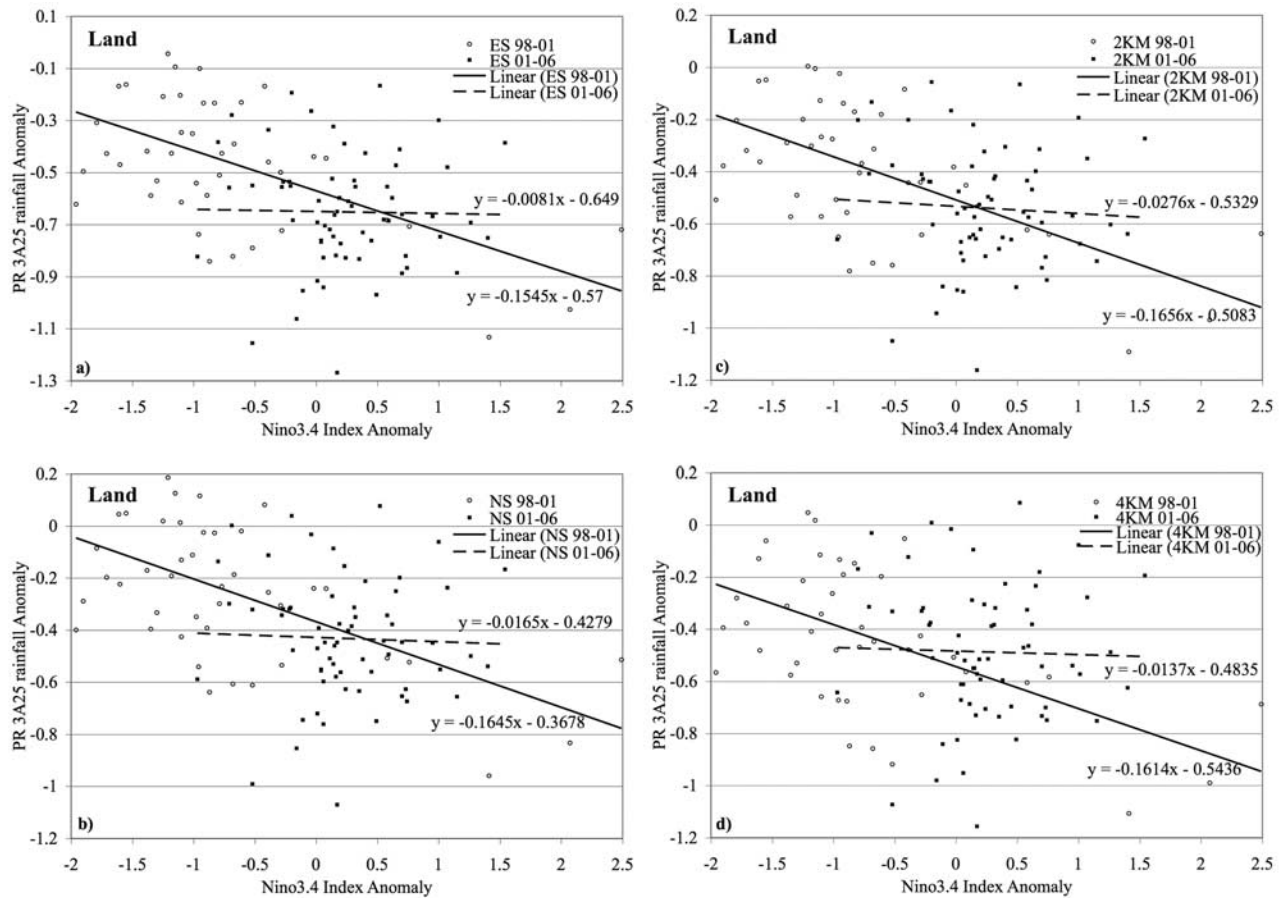


**Figure 3.** The PR rainfall anomalies (mm/d) over the tropical land (25°S–25°N) versus Nino3.4 index at (a) estimated surface, (b) near surface, (c) 2 km, and (d) 4 km.

from the ES to 4 km level). In other words, compared to tropical ocean, the rainfall anomalies over tropical land have little statistical difference from the preboost period to postboost period at all of the analyzed levels from the ES to 4 km (Figure 3). Therefore, no adjustment is made for PR rainfall during the postboost period over tropical land. The possible causes of the difference over land and ocean are still under investigation by the PR algorithm developers. The relative lack of shallow rainfall over land may limit the impact of the boost there because the missing shallow rain due to increased clutter height above the surface is one main contributor to the postboost decrease.

[15] On the basis of the analyses shown in this section, the postboost period PR rainfall is adjusted by adding 6.5, 6.0, and 1.0% to the monthly PR rainfall data over the ocean at the ES, NS, and 2 km level, respectively. No adjustment is made for data over land or at and above the 4 km level. If one calculates the before and after boost differences without taking into account the ENSO effect, the differences are 4.4, 3.8, and 0.0% for the three altitudes, respectively. This small difference between the sets of differences indicates the impact of using the ENSO information. The ENSO effect is certainly secondary to the orbit altitude shift effect but is estimated to be one quarter to one third of the total boost effect by this analysis. Very recent simulations of boost effects on PR data (S. Shimizu, personal communication,

2008) indicate an expected 5.8% impact for ES values (ocean and land combined). This is very comparable to the 6.5% in this study, although our value is for ocean only.

#### 4. Relations Between Monthly Rainfall and Surface Temperature

[16] The relationships between variations of tropical rainfall and surface temperature can now be examined with the adjusted PR information and that from the TMI passive microwave instrument (for which no adjustment was needed). We will first examine the relations between mean ocean rainfall and mean ocean temperature, or mean SST. Then results with regard to precipitation over land are described. Finally, we will examine the relations between variations of total tropical precipitation (ocean plus land) and variations of mean tropical surface temperature (ocean SST plus land surface air temperature). This last combination of total tropical rain versus combined land and ocean temperature is critical to understanding how the tropics operate as a whole.

[17] The positive correlation between SST and the rainfall measured by satellite passive microwave observations is well established [Soden, 2000; Berg et al., 2002; Adler et al., 2003b; Robertson et al., 2003]. Figure 4 shows the time history of the ocean rainfall anomalies during the TRMM

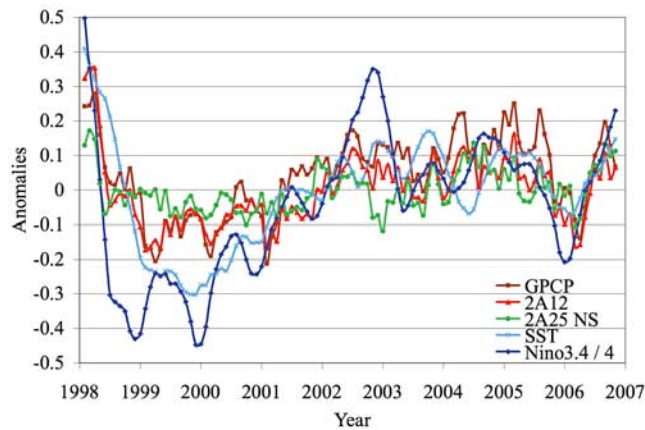


**Figure 4.** Time series of ocean rainfall anomalies (mm/d) from GPCP, TRMM TMI (2A12), TRMM PR (3A25 near surface), ocean mean SST anomalies, and Nino3.4 index anomalies (divided by 4).

period, along with the Nino3.4 index and the mean tropical ocean SST anomaly. It gives a sense of the positive correlation with the central Pacific Ocean ENSO (Nino3.4) index. Also, there is general agreement between the mean ocean-wide SST and mean rainfall variations for the selected products during the period, especially at longer time scales, although the correlation between SST and rain is weaker than when just the central Pacific Ocean values (Nino3.4) are used. The PR NS data show smaller amplitudes than those from the passive microwave observations.

[18] The variations of monthly rainfall measurements from TRMM (including TMI and PR at different levels) and GPCP against the variation of mean SST in the tropical region ( $25^{\circ}\text{S}$ – $25^{\circ}\text{N}$ ) are displayed in Figure 5. As expected, tropical ocean rainfall is positively correlated with mean ocean SST (Figures 5a and 5b). The comparison of the slopes among the TRMM TMI, TRMM PR (at different levels), and GPCP rainfall is listed in Table 2. Over the ocean, GPCP and TRMM TMI (2A12) rainfall data have large and similar slopes against SST anomalies (about  $15\%/^{\circ}\text{C}$ ). The good agreement between GPCP and TRMM TMI rainfall is not a surprise because the satellite instrument driving both data sets is a satellite microwave imager. However, the monthly rainfall anomalies derived from the TRMM PR (3A25) exhibit very different slopes against the SST anomalies at the different levels over the ocean. At lower levels, including ES, NS, and the 2 km level, the linear regression lines of monthly rainfall anomalies are relatively flat (about  $2$ – $4\%/^{\circ}\text{C}$ ). The rainfall intensity derived from TRMM PR decreases significantly from the lowest altitudes, through 2 to 4 km, and farther to 6 km. But percentagewise, the monthly rainfall at 4 and 6 km is more sensitive to SST, showing linear regression lines with larger slopes. One interpretation of this observation is that the rainfall resulting from the deep convection over the ocean is more controlled by the variation of SST. The reason for the different relationships of SST anomalies and the rainfall anomalies derived from microwave imager and precipitation radar is still unclear. One possibility is the difference between radiometer and radar in the physical principles for sensing rainfall. Radar measurements involve only the

backscattering and attenuation of microwaves caused by the hydrometeor at a certain level. Radiometric measurements, however, correspond to an integration of the liquid water in the whole column of the atmosphere. The surface rainfall is estimated from this column of liquid water in the passive microwave estimation techniques. From Figures 5a and 5b, one can see that a vertical integration of the PR slopes at different altitudes might produce a slope comparable with that of the passive microwave observations. It is also possible that attenuation correction deficiencies may limit the lowest level of radar retrievals, especially for deep convective systems. In summary, the ocean surface temperature to ocean rain relationship established with passive microwave observations is not clearly supported by the TRMM PR data.

[19] The relation between land rainfall and ocean mean SST has a negative slope (Figures 5c and 5d), except for PR at 6 km. The regression lines for TRMM TMI and TRMM PR rainfall below 4 km have a range of slope from  $-18$  to  $-14\%/^{\circ}\text{C}$ , while the regression line for GPCP rainfall shows a somewhat deeper slope at  $-26\%/^{\circ}\text{C}$ . The flat regression line for PR at 6 km may imply that although the rainfall over land has a negative correlation with SST, the deep convection over land may have a weaker connection to SST. The negative correlation between SST and land precipitation is also documented in many studies focusing on the variations of ENSO-related SST and precipitation [e.g., *Ropelewski and Halpert, 1996; Trenberth and Caron, 2000*]. It is interesting to note that the obvious disagreement between TRMM PR and TMI rainfall related to the ocean mean SST is not seen over land. This could be related to the following reasons: (1) there is a difference in TRMM PR and TMI algorithms over ocean and over land; (2) the TRMM PR algorithm tends to miss part of shallow rainfall events, and rainfall over land from shallow clouds is a smaller fraction of the total precipitation than over ocean.

[20] When the ocean rain and land rain are combined and the relation between total tropical rain and ocean SST is examined (Figures 5e and 5f), the slopes are generally reduced because of the compensating effects of the land and ocean rain anomalies. However, a positive slope between ocean temperature and tropical rainfall still is present for the passive microwave observations (GPCP and TMI) and for PR observations above 2 km. The magnitude of the slope (see Table 2) is about  $6\%/^{\circ}\text{C}$ . This positive slope is in general agreement with similar calculations done with GPCP tropical rain trend estimates by *Gu et al. [2007]* and *Wentz et al. [2007]* and modeling simulations by *Su et al. [2003]*. However, the PR-based slopes at altitudes 2 km and below are slightly negative, thereby failing to confirm even the sign of the relation. Again, this might be related to attenuation problems with PR retrievals, or it might be related to complicated vertical structure relations as discussed before.

[21] To complete this temperature-rainfall relation exercise, the mean ocean SST is combined with the land temperature information, and that combined surface temperature is compared with the total land plus ocean precipitation anomalies. Results are presented in Figure 6 and Table 3. Since the land surface temperature tends to vary somewhat synchronously with mean ocean temperature during ENSO variations [*Yulaeva and Wallace, 1994*], we

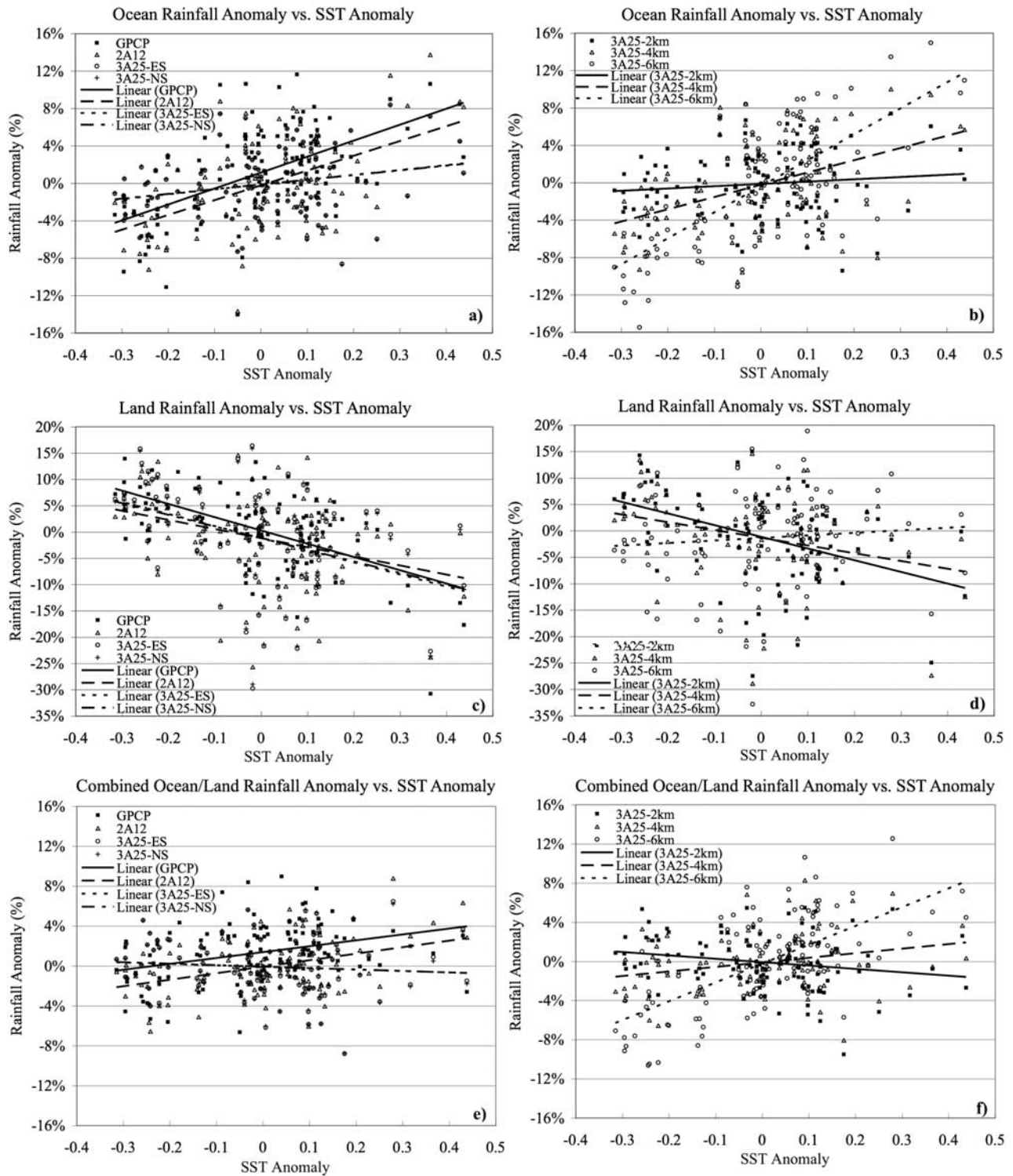


**Figure 5.** Percentage of monthly rainfall anomalies versus SST anomalies ( $^{\circ}\text{C}$ ) in (a, b) tropical ocean, (c, d) tropical land, and (e, f) total tropical region.

expect the results to be similar to using only ocean-wide SST, which they are. Even the magnitudes of the slopes are very similar. Figure 6 is the culmination of this exercise, as it shows the final surface temperature-rainfall relations over the tropics based on current TRMM products, with a comparison with GPCP. Again, the TMI-based estimate

agrees with the GPCP estimate with an approximate value of  $5\text{--}6\%/^{\circ}\text{C}$ . The PR-based value at 4 km altitude is similar ( $4\%/^{\circ}\text{C}$ ), but the ES, NS, and 2 km values have negative values. One would not expect a negative slope in the physical relationship between these two variables, so this result may be more likely to signal a problem in the PR

**Table 2.** Slopes of the Linear Regression Lines for TRMM TMI, TRMM PR, and GPCP Monthly Rainfall Anomalies to Sea Surface Temperature Anomalies<sup>a</sup>

	Ocean	Land	Ocean Plus Land
GPCP	16.7	-25.8	5.9
TRMM TMI	15.4	-16.9	6.5
TRMM PR estimated surface	4.4	-16.9	-1.4
TRMM PR near surface	4.3	-16.7	-1.5
TRMM PR 2 km	1.7	-18.3	-3.5
TRMM PR 4 km	11.9	-14.3	4.6
TRMM PR 6 km	26.6	4.8	19.2

<sup>a</sup>TMI, Tropical Rainfall Measuring Mission Microwave Imager; PR, Precipitation Radar. Values are in %/°C.

retrieval. This would take the form of a greater failure to correct enough for attenuation in situations of more intense convection, which are more likely to occur during warm SST periods. Thus, we are left with a mixed set of results as to how interannual variations of surface temperature are related to rainfall variations over the tropics.

### 5. Summary and Conclusions

[22] Rainfall information from TRMM during the 9-year (1998–2006) period enables an independent look at some basic rainfall-temperature relations being derived from a previous data set, e.g., GPCP. The TRMM data also allow for both radar and passive microwave observations to be used.

[23] First, a technique is derived to account for the changes in the radar-based estimates caused by the increase in the TRMM satellite orbit from 350 to 402 km in August 2001. After that increase in altitude, the TRMM PR rainfall data show an apparent drop during the postboost period, especially at the lower levels. A simple technique is developed to adjust the PR monthly rainfall data in the tropics (whole ocean and whole land) during the postboost period, taking into account the impact of ENSO events. On the basis of the relationship between TRMM PR rainfall and the Nino3.4 index, an indicator of ENSO events before and after the boost of TRMM satellite, the postboost period PR rainfall is adjusted by adding 6.5, 6.0, and 1.0% to the monthly PR rainfall data over the ocean at the estimated surface, near surface, and 2 km level, respectively. No adjustment is made for data over land and at or above the 4 km level.

[24] The relationships between the tropical rainfall and surface temperature are then examined with both the TMI and adjusted PR data. Our focus is to use the TRMM rainfall data set, including the PR in comparison to the passive microwave data, to examine its response to surface temperature variation. This exercise is done for ocean rainfall versus SST and, finally, for combined ocean-land rainfall versus combined land-ocean surface temperature. Over ocean and land combined, TRMM TMI (2A12) and GPCP rainfall data have rather similar positive slopes (about 6%/°C), but the PR (3A25) rainfall data slope is near zero (even negative) except at the 4 km level, where the positive slope (4%/°C) approximately matches the passive value. In other words, the surface temperature to rain relationship

established with passive microwave observations is not clearly supported by the TRMM PR data, unless one assumes the 4 km level PR data best represents surface rain variations. The same results hold for ocean rainfall-mean SST relations, with the rainfall-temperature slope being about 15%/°C from the passive microwave observations, but less from the PR data, except for 4 km altitude (12%/°C). The reasons causing the different relationships of surface temperature anomalies and the rainfall anomalies derived from microwave imager and precipitation radar are still unclear. They may be the result of PR retrieval error or inherent passive/active retrieval differences. The apparently nonphysical negative slopes derived for the rain-temperature

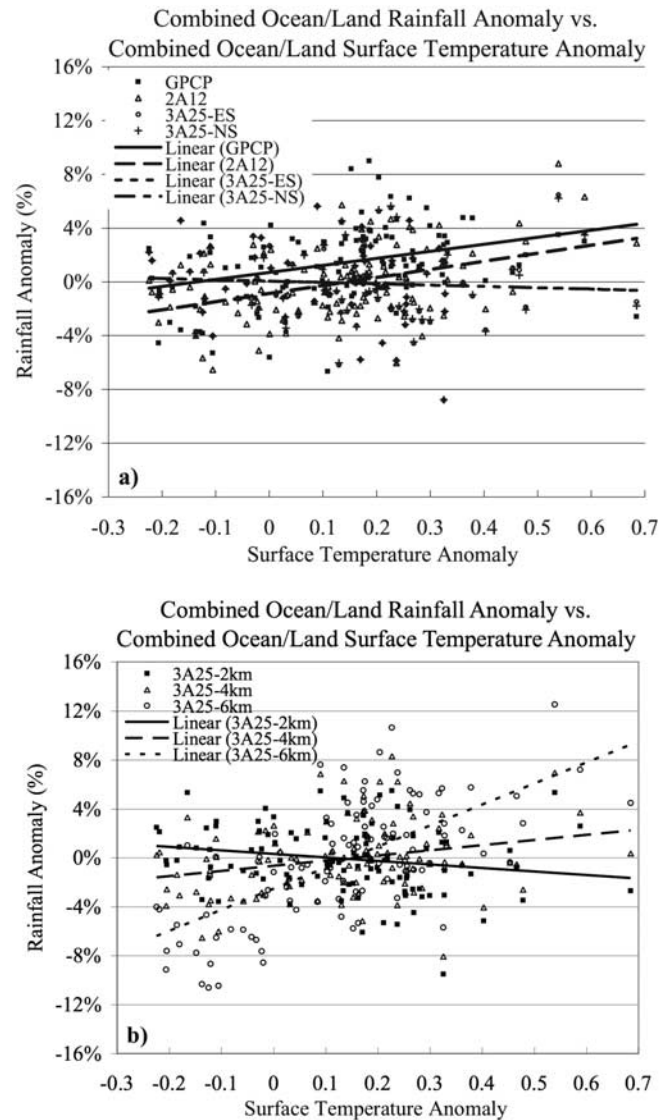


**Figure 6.** Percentage of monthly rainfall anomalies versus surface temperature anomalies (°C) in total tropical region for (a) GPCP, TRMM 2A12, TRMM 3A25 at estimated surface, and TRMM 3A25 at near surface and (b) TRMM 3A25 at 2, 4, and 6 km, from the average of 1979–2006 in the total tropical region. Note that in Figure 6a the regression line for 3A25-ES and 3A25-NS are almost overlapped.

**Table 3.** Slopes of the Linear Regression Lines for TRMM TMI, TRMM PR, and GPCP Monthly Rainfall Anomalies to Surface Temperature Anomalies

	Ocean Plus Land (%/°C)
GPCP	5.3
TRMM TMI	6.0
TRMM PR estimated surface	-1.0
TRMM PR near surface	-1.0
TRMM PR 2 km	-2.9
TRMM PR 4 km	4.2
TRMM PR 6 km	17.2

relations over the total tropics for the lowest levels of the PR data may indicate that the retrieval method is failing to capture variations in rain profiles near the surface under varying large-scale conditions. Further research is needed to advance the use of TRMM data in this regard.

[25] With the continuation of TRMM through the next few years, to be followed by the Global Precipitation Measurement (GPM) mission with a similar radar, continued improvement of the rain algorithms themselves and the techniques to use the information will be valuable in diagnosing rainfall-temperature and other important relations on the climate scale.

[26] **Acknowledgments.** The authors would like to thank David Bolvin for providing the gridded TRMM monthly rainfall data. The constructive suggestions by three anonymous reviewers also improved the presentation of this study. This research was sponsored by NASA under its Precipitation Measurement Missions (TRMM and GPM) program, led by Ramesh Kakar of NASA headquarters, and by the NASA Energy and Water Cycle Study (NEWS), led by Jared Entin.

## References

- Adler, R. F., et al. (2003a), The version 2 Global Precipitation Climatology Project (GPCP) monthly precipitation analysis (1979-present), *J. Hydrometeorol.*, *4*, 1147–1167, doi:10.1175/1525-7541(2003)004<1147:TVGPCP>2.0.CO;2.
- Adler, R. F., C. Kummerow, D. Bolvin, S. Curtis, and C. Kidd (2003b), Status of TRMM monthly estimates of tropical precipitation, *Meteorol. Monogr.*, *29*(51), 223–234.
- Berg, W., C. Kummerow, and C. A. Morales (2002), Differences between east and west Pacific rainfall systems, *J. Clim.*, *15*, 3659–3672, doi:10.1175/1520-0442(2002)015<3659:DBEAWP>2.0.CO;2.
- Chiu, L. S., and A. T. Chang (2000), Oceanic rain column height derived from SSM/I, *J. Clim.*, *13*, 4125–4136, doi:10.1175/1520-0442(2000)013<4125:ORCHDF>2.0.CO;2.
- Curtis, S., and R. F. Adler (2003), Evolution of El Niño-precipitation relationships from satellites and gauges, *J. Geophys. Res.*, *108*(D4), 4153, doi:10.1029/2002JD002690.
- Gu, G., R. F. Adler, G. Huffman, and S. Curtis (2007), Tropical rainfall variability on interannual-to-interdecadal and longer time scales derived from the GPCP monthly product, *J. Clim.*, *20*, 4033–4046, doi:10.1175/JCLI4227.1.
- Hansen, J., R. Ruedy, J. Glasco, and M. Sato (1999), GISS analysis of surface temperature change, *J. Geophys. Res.*, *104*, 30,997–31,022, doi:10.1029/1999JD900835.
- Huffman, G. J., R. F. Adler, P. Arkin, A. Chang, R. Ferraro, A. Gruber, J. Janowiak, A. McNab, B. Rudolf, and U. Schneider (1997), The Global Precipitation Climatology Project (GPCP) combined precipitation dataset, *Bull. Am. Meteorol. Soc.*, *78*, 5–20, doi:10.1175/1520-0477(1997)078<0005:TGPCPG>2.0.CO;2.
- Iguchi, T., T. Kozu, R. Meneghini, J. Awaka, and K. Okamoto (2000), Rain-profiling algorithm for the TRMM precipitation radar, *J. Appl. Meteorol.*, *39*, 2038–2052, doi:10.1175/1520-0450(2001)040<2038:RPAFFT>2.0.CO;2.
- Kummerow, C., et al. (2000), The status of the Tropical Rainfall Measuring Mission (TRMM) after two years in orbit, *J. Appl. Meteorol.*, *39*, 1965–1982, doi:10.1175/1520-0450(2001)040<1965:TSOTTR>2.0.CO;2.
- Kummerow, C., et al. (2001), The evolution of the Goddard Profiling Algorithm (GPROF) for rainfall estimation from passive microwave sensors, *J. Appl. Meteorol.*, *40*, 1801–1820, doi:10.1175/1520-0450(2001)040<1801:TEOTGP>2.0.CO;2.
- Kwiatkowski, J., Y. Ji, and J. Stout (2007), TRMM analysis toward algorithm improvement, paper presented at NASA Precipitation Measurement Missions (PMM) Science Team Meeting, Atlanta, Ga., 7–10 May.
- Reynolds, R. W., N. A. Rayner, T. M. Smith, D. C. Stokes, and W. Wang (2002), An improved in situ and satellite SST analysis for climate, *J. Clim.*, *15*, 1609–1625, doi:10.1175/1520-0442(2002)015<1609:AIIASAS>2.0.CO;2.
- Robertson, F. R., D. E. Fitzjarrald, and C. D. Kummerow (2003), Effects of uncertainty in TRMM precipitation radar path integrated attenuation on interannual variations of tropical oceanic rainfall, *Geophys. Res. Lett.*, *30*(4), 1180, doi:10.1029/2002GL016416.
- Robertson, F. R., D. E. Fitzjarrald, and H. I. Lu (2007), Recent water and energy cycle variations as seen from TRMM and other sensors, paper presented at NASA Precipitation Measurement Missions (PMM) Science Team Meeting, Atlanta, Ga., 7–10 May.
- Ropelewski, C. F., and M. S. Halpert (1996), Quantifying Southern Oscillation-precipitation relationships, *J. Clim.*, *9*, 1043–1059, doi:10.1175/1520-0442(1996)009<1043:QSOPR>2.0.CO;2.
- Simpson, J., (Ed.) (1988), TRMM: A satellite mission to measure tropical rainfall, report of the Science Steering Group, 94 pp., NASA Goddard Space Flight Cent., Greenbelt, Md.
- Soden, B. J. (2000), The sensitivity of the tropical hydrological cycle to ENSO, *J. Clim.*, *13*, 538–549, doi:10.1175/1520-0442(2000)013<0538:TSOTTH>2.0.CO;2.
- Su, H., D. Neelin, and J. E. Meyerson (2003), Sensitivity of tropical tropospheric temperature to sea surface temperature forcing, *J. Clim.*, *16*, 1283–1301, doi:10.1175/1520-0442(2003)16<1283:SOTTTT>2.0.CO;2.
- Takahashi, N., and T. Iguchi (2004), Estimation and correction of beam mismatch of the precipitation radar after an orbit boost of the Tropical Rainfall Measuring Mission satellite, *IEEE Trans. Geosci. Remote Sens.*, *42*, 2362–2369, doi:10.1109/TGRS.2004.837334.
- Trenberth, K. E., and J. M. Caron (2000), The Southern Oscillation revisited: Sea level pressures, surface temperatures, and precipitation, *J. Clim.*, *13*, 4358–4365, doi:10.1175/1520-0442(2000)013<4358:TSORSL>2.0.CO;2.
- Wentz, F. J., L. Ricciardulli, K. Hilburn, and C. Mears (2007), How much more rain will global warming bring?, *Science*, *317*, 233–235, doi:10.1126/science.1140746.
- Yulaeva, E., and J. M. Wallace (1994), The signature of ENSO in global temperature and precipitation fields derived from the microwave sounding unit, *J. Clim.*, *7*, 1719–1737, doi:10.1175/1520-0442(1994)007<1719:TSOEIG>2.0.CO;2.

R. F. Adler, G. Gu, and J.-J. Wang, Laboratory for Atmospheres, NASA Goddard Space Flight Center, Code 613.1, Greenbelt, MD 20771, USA. (jjwang@agnes.gsfc.nasa.gov)